

Visual Movement Detection Under Light- and Dark-Adaptation in the Fly, *Musca domestica*

Bernward Pick † and Erich Buchner *

Max-Planck-Institut für biologische Kybernetik, Spemannstrasse 38, D-7400 Tübingen, Federal Republic of Germany

Accepted August 3, 1979

Summary. Visual movement detection has been investigated both under photopic and scotopic light conditions by measuring the optomotor turning responses of walking flies, *Musca domestica*. From the data it is concluded that the spatial sampling pattern underlying movement detection changes with the average stimulus brightness. At high luminance nearest-neighbour interactions clearly dominate whereas at very low light intensities interactions between receptors having one, two and three times the minimum angular separation contribute with about equal strength to the response (Figs. 6, 7). This change in the spatial interaction pattern may be based on neuronal recruitment of wide-angle movement detectors at low light levels or, alternatively, on neural pooling of signals from neighbouring receptors prior to the movement-specific interactions. Both mechanisms may provide a gain in absolute light sensitivity at the cost of spatial acuity.

The temporal properties of movement detection also change with stimulus brightness. High grating speeds are detected less efficiently at low luminance (Fig. 3). These temporal changes may be attributed to equivalent changes in the photoreceptor responses.

Negative optomotor responses may be elicited by a pair of test stimuli separated in visual angle by about 15° corresponding to 7–8 rows of ommatidia (Figs. 9, 10). This unexpected behaviour is suggested to reflect the influence of lateral inhibition which extends, in the periphery of the visual system, with de-

creasing strength over a range of at least 5 rows of ommatidia. Movement-specific interactions on the other hand do not appear to extend beyond 4–5 rows of ommatidia.

Introduction

The aerobic performance of rapidly flying insects reflects an elaborate system of visual movement detection. It has been shown that the *spatial* resolution, as set by the receptor density in the compound eyes, is fully utilized (Götz, 1964; Eckert, 1973; Buchner, 1976). The excellent *temporal* properties of this processing are illustrated by the finding that the motor response may follow the movement stimulus within less than 25 ms (Land and Collett, 1974; Reichardt and S. Buchner, pers. comm.; Reichardt and Poggio, 1976; Collett and Land, 1978.) Such fast and “fine-grain” processing, however, has disadvantages that become apparent under dim light conditions, when the light signals in individual receptors become too noisy to allow unequivocal motor commands within a limited interval of processing time (Fermi and Reichardt, 1963; Snyder, 1977).

Ultimately, the absolute light sensitivity of the photoreceptors is limited by the maximum effective optical aperture. Once this has been fully utilized, additional mechanisms of dark adaptation may perform spatial, temporal and/or chromatic integration only *at the cost* of spatial acuity, temporal and/or chromatic resolution. Visual psychophysics provides ample evidence that temporal and spatial summation are mechanisms of dark adaptation in the human visual system (cf. Barlow, 1972).

In the invertebrate retina and more specifically also in fly photoreceptors, three relevant adaptational mechanisms have been discussed. Firstly, temporal

* Shortly before completion of the manuscript Dr. Bernward Pick died unexpectedly at the age of 34. We who knew him were deeply shocked by his death

Abbreviations: *R1-6*, the six peripheral receptors in a fly's ommatidium; *R7/8*, the two central receptors in a fly's ommatidium; $\Delta\rho$, half width of angular sensitivity function; $\Delta\phi^*$, angle between optical axes of neighbouring rows of ommatidia ($\sqrt{3}/2$ interommatidial angle); λ , spatial wavelength of periodic grating; m_{rec} , light modulation in a receptor

integration gradually increases with decreasing stimulus luminance (Zettler, 1969). Secondly, the visual-field size of the individual receptor may increase at low luminance, i.e., *spatial acuity* is sacrificed. In flies, however, the visual field diameter or acceptance angle $\Delta\rho$ has been found to change very little with ambient luminance (*Musca*: Scholes, 1969; *Calliphora*: Hardie, 1979). Thirdly, in analogy to the vertebrate retina, it was proposed that flies may use their different receptor types R1–6 and R7/8 for vision at low and high light intensities, respectively (Kirschfeld and Franceschini, 1968; Eckert, 1973). A manifestation of this specialization has not yet been clearly established for any behaviour so far studied (cf. Heisenberg and Buchner, 1977).

The present paper provides evidence for an adaptational mechanism beyond the level of the retina. We find that movement detection at low light levels is facilitated at the cost of *spatial acuity*. Optomotor responses of *Musca* under photopic and scotopic light conditions are compared. When the temporal properties of the response are taken into account, the data show that *scotopic* movement detection is based upon an extended spatial sampling pattern involving more than nearest-neighbour interactions. This spatial extension of movement-specific interactions may well be achieved by pooling the signals from neighbouring receptors prior to the movement-specific interaction. The relationship between illumination and threshold acuity in a movement-sensitive interneuron in *Lucilia* has been recently proposed to be partly due to an adaptational mechanism of this kind (Dvorak and Snyder, 1978). The extended spatial sampling scheme described here may account for the reduced acuity of certain *Drosophila* mutants (Heisenberg and Götz, 1975; Heisenberg and Buchner, 1977) and of *Musca* at threshold luminance (Eckert, 1973). The implications of this mechanism of dark adaptation for vision at low light levels are discussed.

Methods

Adult female *Musca domestica*, from 4 to 10 days post-emergence, were used in the experiments. Under light anesthesia by carbon dioxide or ether the head was secured to the thorax and the wings were cut. The ocelli were covered with black paint. Turning responses of the walking animal which was rigidly suspended from a micromanipulator were recorded either by means of a y-maze globe (Hassenstein, 1951) or a small styrofoam sphere (Buchner, 1976). The quotient $(r-l)/(r+l)$ of right minus left and right plus left decisions on the y-maze globe, as well as the quotient $(\text{rev. } r/\text{rev. } f)$ of the revolutions of the styrofoam sphere about the vertical axis (*rotation*) and a horizontal axis perpendicular to the fly's body (*forward walk*) both represent quantitative measures of the turning tendencies of the flies. Figures 3 and 5 through 10 display the differences of the turning responses to clockwise and counter-

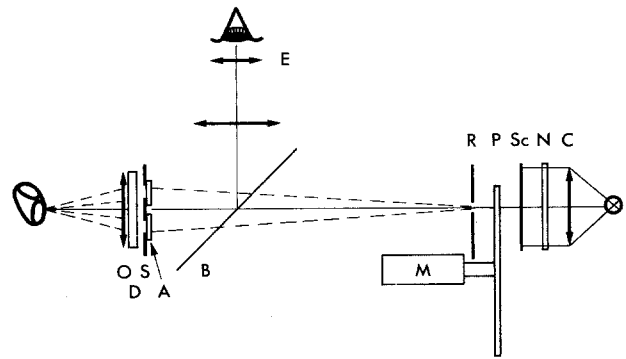


Fig. 1. Experimental set-up used to project two bright stripes onto the fly's compound eye. The rectangular diaphragm *R* is homogeneously illuminated by a tungsten lamp (Leitz Nimi, 6 V 15 W) with condenser *C*, a broad-band blue filter (Schott BG 23), neutral density glass filters *N* (Schott NG 3, NG 4, NG 5) and a translucent screen *Sc*. By means of the objective *O* (Leitz UMK 32, n.a. 0.40, $f=8.5$ mm) the diaphragm *R* is focussed on the center of the fly's eye such that the "deep pseudopupil" is fully illuminated. Diaphragm *S*, which consists of two parallel slits may be rotated in the back focal plane of *O* in order to align the slits in parallel with the vertical rows of visual elements. Shape, width and separation of the two slits could be adjusted as required for the various stimulus configurations of Figs. 4, 9 and 10 by inserting different diaphragms *S*. The brightness of the two slits is sinusoidally modulated at a frequency of 2 Hz by rotating a polarizer *P* behind the two analyzing filters *A* (Käsemann, Polarexfolie PW-64). The angle between the optical axes of the two analyzers determines the phase $\Delta\Omega$ between the light signals from the two slits. The pattern is depolarized by a quartz depolarizer *D* (Halle, lyot-depolarizer 6 mm). There is no background illumination. After the fly has been positioned and the diaphragm *S* aligned with the rows of visual elements, the beam-splitter pellicle *B* and the eyepiece *E* are removed

clockwise movement, i.e., the direction-sensitive portion of the optomotor response (Reichardt and Poggio, 1976).

Three types of visual stimuli were used: (1) A vertically-striped precision cylinder (diameter 10 cm) was rotated at constant speed in clockwise or counterclockwise direction around the fly which was centered to the axis of the cylinder. Translucent and ground plexiglas provided spatial filtering such that the spatial intensity distribution of the stripes approximated a sine wave with the amplitude of the harmonics not exceeding 10% of the amplitude of the fundamental pattern wavelength λ . 76% contrast and 2 Hz contrast frequency (=number of pairs of black and white stripes passing a fixed point per s) were used for all striped patterns. A stationary black masking cylinder (diameter 7.5 cm) delimited the visual field in the vertical direction to $\pm 10^\circ$ above and below the equatorial plane of the fly and to $\pm 120^\circ$ laterally with respect to forward direction. Homogeneous illumination was provided from the outside by tungsten lamps through broad-band blue filters (Schott BG 23). The intensity was adjusted by neutral-density glass filters (Schott, NG filters). The UV-content of the stimuli was very low, color-specific adaptation phenomena are not to be expected. (2) A precision sine-wave grating (amplitude of harmonics less than 1% of fundamental) of variable spatial wavelength was projected onto a circular portion (diameter 40°) of the upper frontal visual field of one eye by means of a microscope objective. The orientation of the stripes was aligned in parallel with the vertical rows of the hexagonal receptor array (for details see Buchner, 1976; Buchner et al., 1978). (3) Two bright stripes were

projected through a microscope objective onto two arrays of visual elements.¹ The luminance of each stripe was sinusoidally modulated with an adjustable phase shift $\Delta\Omega$ between the two signals to induce apparent ("phi-") movement front-to-back or back-to-front (Fig. 1). Like the gratings described above these flickering stripes produce sinusoidal light signals in the photoreceptors. The significant advantages of the local stripes over an extended grating are: (i) By the two stripes a common phase shift $\Delta\Omega$ is generated for all movement-specific interactions stimulated. For a moving grating with spatial wavelength λ , on the other hand, $\Delta\Omega$ depends on the spatial separation $n \cdot \Delta\varphi^*$ of two interacting receptors ($n=1, 2, 3 \dots$) according to $\Delta\Omega = 2\pi n \cdot \Delta\varphi^* / \lambda$. The angle $\Delta\varphi^*$ represents the smallest effective sampling base of the periodic receptor array (cf. inset Fig. 6). Thus if more than one sampling base is involved in movement detection there is no longer a common phase shift $\Delta\Omega$ for all movement-specific interactions. (ii) The temporal modulation of light flux in the receptors stimulated by local stripes changes very little when $\Delta\Omega$ is varied whereas for moving stripes it depends on λ according to the modulation transfer function (eq. (2); below). The flickering stripes are therefore convenient to investigate the movement-specific mechanism itself without interference by modulation transfer and spatial interaction problems. As all three types of stimuli employ tungsten sources and broad-band blue filtering, luminance scales as calibrated by means of a lux meter (Gossen) are directly comparable. The threshold of screening pigment migration in R1-6 of *Musca* under these conditions has previously been measured to lie near 1 cd/m² (Heisenberg and Buchner, 1977).

In the experiments using moving sine-wave gratings for stimulation the dependence of the direction-sensitive turning responses R on spatial frequency $1/\lambda$ is analyzed according to the following formula

$$R(1/\lambda) = \left[\frac{D \cdot m_{rec}}{1 + D \cdot m_{rec}} \right]^2 \cdot \sum_n B_n \cdot \sin \frac{2\pi n \Delta\varphi^*}{\lambda}. \quad (1)$$

The Fourier sine series in this expression has been derived by theoretical considerations on movement detection systems (Poggio and Reichardt, 1973). In its particular formulation Eq. (1) has previously been shown to adequately describe contrast and spatial-frequency dependence of direction-sensitive movement responses of *Drosophila* at various light levels (Buchner, 1976; Heisenberg and Buchner, 1977; Buchner et al., 1978). Eq. (1) is also in agreement with similar contrast dependence data on *Musca* (Eckert, 1973). The expression $D \cdot m_{rec} / (1 + D \cdot m_{rec})$ is proposed to describe the amplitude of neuronal input signals to the movement detectors as a function of light modulation in the receptors m_{rec} . Harmonics of the temporal stimulus frequency generated by adaptational nonlinearities are assumed to be negligible. The above function is illustrated in Fig. 2 for various values of the luminance-dependent parameter D . Near threshold ($D \ll 1$) the function is approxi-

mately linear with the modulation m_{rec} whereas at higher luminance ($D \gg 1$) saturation sets in already at low values of the modulation m_{rec} . Thus the parameter D allows for range setting in receptors and neurons distal to the movement-specific interaction. If the mechanism of movement detection corresponds to the broad class of multiplicative (or second-order or correlation-like) models (Poggio and Reichardt, 1973) the above expression must be raised to the second power, as in Eq. (1). If Eq. (1) holds, the value of D at a particular luminance may then be determined by measuring the behavioural response R as a function of pattern contrast $\Delta I/\bar{I}$. The latter is related to the light modulation m_{rec} by the receptor modulation transfer function:

$$m_{rec} = \Delta I/\bar{I} \cdot \exp \left\{ \frac{-\pi^2}{4 \cdot \ln 2} \left(\frac{\Delta\rho}{\lambda} \right)^2 \right\}. \quad (2)$$

The exponential factor accounts for the well-known attenuation of high spatial frequencies and depends on the receptor acceptance angle $\Delta\rho$ (e.g., Götz, 1964). $\Delta\varphi^*$ represents the angular separation of neighbouring vertical rows of visual elements. The interaction coefficients $B_1, B_2, B_3 \dots$ give the movement-specific contributions from pairs of visual elements located in adjacent, adjacent but one, adjacent but two ... vertical rows of visual elements. They may be determined by Fourier analysis of $R(1/\lambda)$.

Results

1. Luminance-Dependent Changes in the Temporal Properties of Movement Detection

The range of optomotorically effective grating speeds (w) changes with the average grating luminance (Fig. 3). The overall shape of the two curves differs particularly at high pattern speeds. A significant response decrement is measured at low pattern luminance for instance at $w/\lambda = 19$ Hz.

Directionality and nonlinear properties of the movement-specific interaction are reflected by the dependence of the response on the temporal phase shift $\Delta\Omega$ between the input signals. To determine whether these properties change with stimulus luminance, turning responses were measured at low light levels using the pair of flickering stripes. Figure 4 shows an approximately sinusoidal dependence on $\Delta\Omega$ similar to that previously observed at high luminance (Pick, 1974). This indicates that direction-sensitive movement detection in *Musca* is well characterized by multiplicative (2nd order nonlinear) 2-channel interaction, irrespective of ambient light level.

¹ A "visual element" represents the eye's functional unit comprising eight receptors which are located in seven neighbouring ommatidia and sample approximately the same spot in visual space (cf. Pick, 1977)

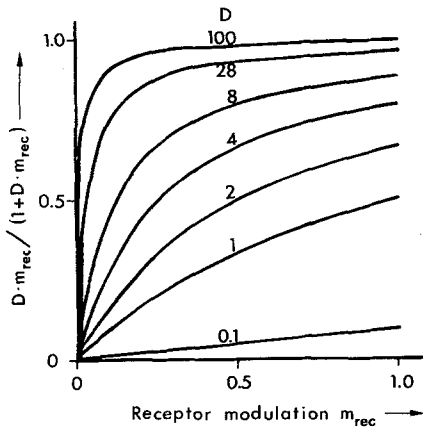


Fig. 2. Proposed dependence of the input signals to neural movement detectors on the light modulation in the receptors m_{rec} . The parameter D depends on the mean stimulus luminance \bar{I} . $D=4$ and $D=28$ are estimates obtained from unpublished contrast dependence measurements of the optomotor response of *Musca* at $\bar{I}=3 \cdot 10^{-3} \text{ cd/m}^2$ and $\bar{I}=100 \text{ cd/m}^2$

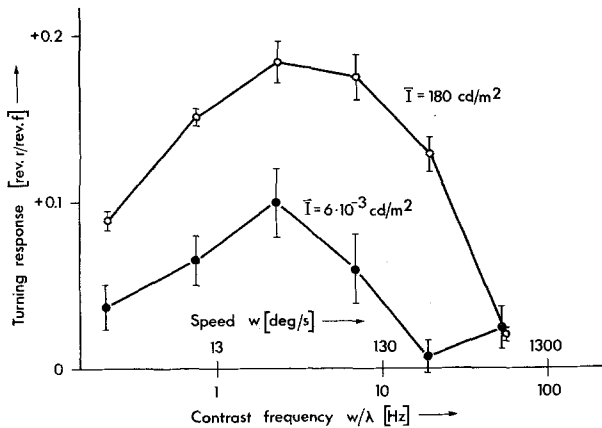


Fig. 3. Optomotor turning response as a function of grating speed at a constant spatial wavelength of $\lambda=13^\circ$. The equivalent scale of "contrast frequency" gives the number of brightness cycles per second in each receptor, i.e. the temporal stimulus frequency. Pattern contrast $\Delta I/\bar{I}$ was 40% (stimulus 2, cf. Methods). Response mean (\pm S.E.M.) from 5 animals

2. Luminance-Dependent Changes in the Spatial Properties of Movement Detection

Turning responses to moving gratings of varying spatial wavelength were measured at and near the luminance threshold (Fig. 5). While fine gratings hardly elicit responses within the first decade above threshold intensity, patterns with $\lambda=45^\circ$, 21° and 90° wave-

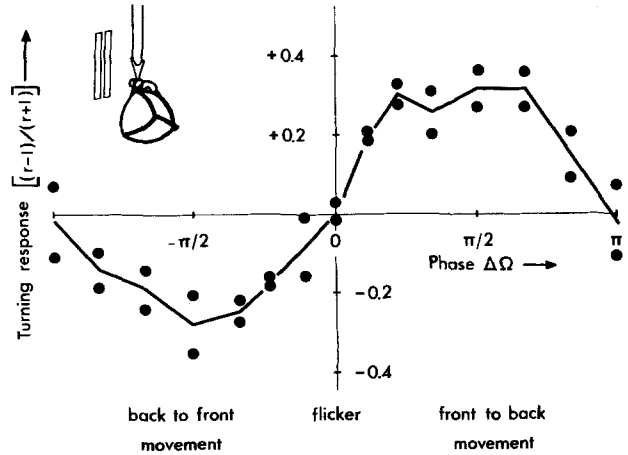


Fig. 4. Turning reactions of a single fly as a function of the phase shift $\Delta\Omega$ between the sinusoidal intensity functions of two vertical stripes (stimulus 3, cf. Methods). The stripes are 1.8° wide and 13° high. Center-to-center separation 3.8° . The stripes are projected about 20° laterally on the equatorial region of the right eye (Fig. 1) and stimulate two vertical rows each consisting of approximately seven visual elements. Mean stimulus luminance $3 \cdot 10^{-3} \text{ cd/m}^2$. Background dark

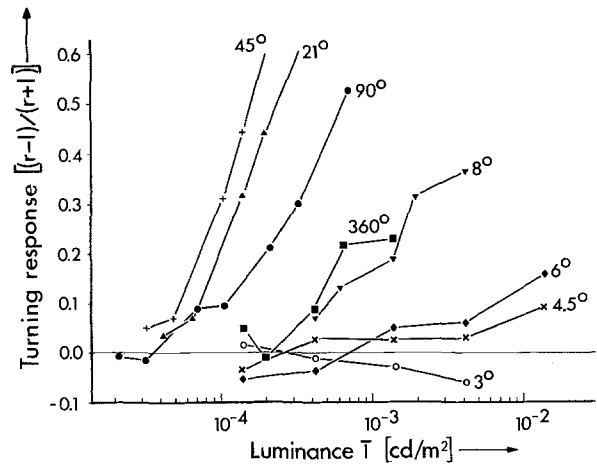


Fig. 5. Optomotor turning response of a single fly. The parameter 45° , 21° , ... denotes the spatial wavelength (λ) of the grating as seen by the fly in the center of the drum. Pattern contrast $\Delta I/\bar{I}=76\%$; contrast frequency $w/\lambda=2 \text{ Hz}$ (stimulus 1, cf. Methods). Below a luminance of 10^{-4} cd/m^2 the reactions to gratings of 3° to 8° wavelength scatter around zero and have therefore not been measured with every test run

length are most effective. From such threshold curves the spatial-frequency response $R(1/\lambda)$ at a criterion intensity near threshold can be safely interpolated without interference by saturation artifacts. The thus resulting Fig. 6 has one narrow long-wavelength peak although the theoretically detectable range of grating wavelengths extends to the resolution limit near 4° . This shape of $R(1/\lambda)$ significantly differs

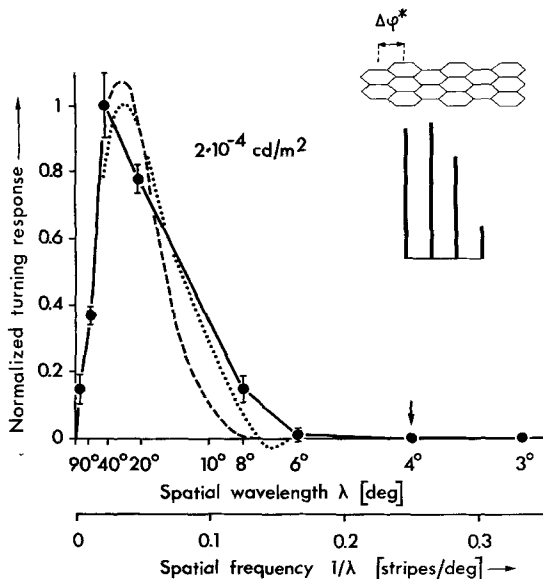


Fig. 6. Turning responses (R) measured as in Fig. 5 and plotted at a criterion intensity close to threshold ($2 \cdot 10^{-4}$ cd/m²) over spatial frequency ($1/\lambda$). Mean from 5 flies (\pm S.E.M.) normalized to equal peak response. An approximation of $R(1/\lambda)$ according to Eq. (1) with $\Delta\rho=2.4^\circ$ and $D \ll 1$ (threshold intensity) is given by the dotted curve. The first four interaction coefficients B_{1-4} which relate to the sampling bases $\Delta\varphi^*$, $2\Delta\varphi^*$, $3\Delta\varphi^*$ and $4\Delta\varphi^*$ are 0.40, 0.42, 0.32, 0.11, respectively, as shown in the figure inset. Using the normalized interaction coefficients B_{1-4} valid at high grating luminance (1, 0.56, 0.20, 0.10, Fig. 7b) and varying the acceptance angle $\Delta\rho$ the best fit to the data with $D \ll 1$ is obtained for $\Delta\rho=6^\circ$ (dashed curve). The spatial resolution limit $2\Delta\varphi^*$ is about 4° (arrow)

from that obtained from *Drosophila* at high luminance (Buchner, 1976). We have therefore directly measured spatial-frequency functions $R(1/\lambda)$ under otherwise identical conditions at high and low grating luminance.

At a luminance of $2 \cdot 10^{-4}$ cd/m² (Fig. 6) small patterns presented to only one eye (stimulus 2) did not elicit responses large enough to yield meaningful interaction coefficients. The low-luminance data were therefore measured at $3 \cdot 10^{-3}$ cd/m² (Fig. 7a). Note that there is no significant difference in the shape of the curves in Figs. 6 and 7a when normalized to equal peak response.

The different shapes of the response functions at $3 \cdot 10^{-3}$ cd/m² (Fig. 7a) and 100 cd/m² (Fig. 7b) indicate a luminance-dependent modification of the interaction scheme. Reduced responses elicited by low-contrast patterns at high luminance were measured for comparison. Again there is no indication of saturation for large responses. Details on the calculation and significance of the interaction coefficients B_1, B_2, \dots which are shown as insets to each figure will be given in the Discussion. The large 1st coefficient of Fig. 7b indicates that interactions between neighbour-

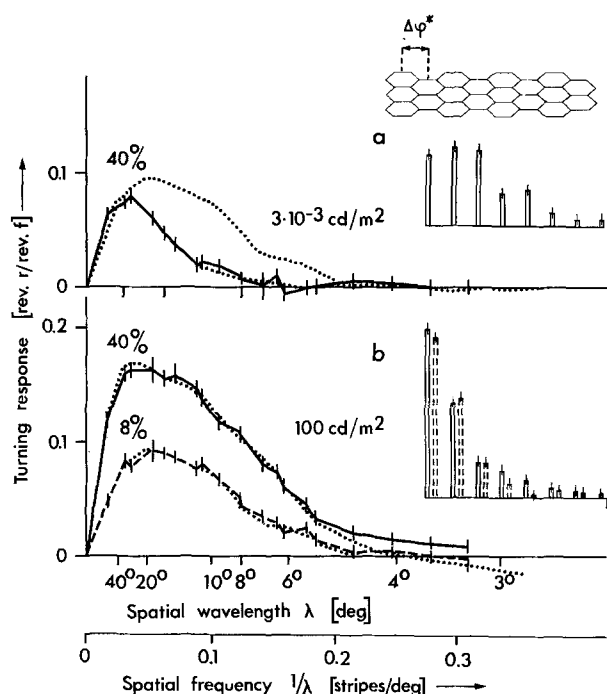


Fig. 7a and b. Spatial-frequency response $R(1/\lambda)$ at low (a) and high (b) pattern luminance measured directly by varying λ . The speed w was adjusted to keep the contrast frequency w/λ constant at 2 Hz (stimulus 2). Mean from 5 flies (\pm S.E.M.). Analyzing the data according to Eq. (1) and allowing for 8 non-zero Fourier coefficients $B_1 \dots B_8$ one obtains the coefficients displayed as columns in the insets and the dotted curves as the best fit to the data in the sense of least square errors. Note in Fig. 7b that reduction of the grating contrast from 40% to 8% attenuates the responses in accordance with Eq. (1) but does not modify the shape of the curve or the sizes of the Fourier coefficients (dashed). The error bars of the interaction coefficients are estimates only for the relative variation of the coefficients in each inset since they were calculated from the errors of the corresponding turning responses ignoring possible errors of the values of D and $\Delta\rho$ in Eqs. (1) and (2). The absolute sizes of the coefficients in a and b cannot be compared as long as D is not known accurately (cf. Discussion). The low-contrast response curve is displayed also in a to illustrate the different shape of the low-luminance curve

ing rows of visual elements clearly dominate at high luminance whereas at low luminance interactions between neighbouring, neighbouring-but-one and neighbouring-but-two rows contribute with about equal weight to the response (1st, 2nd and 3rd coefficient Figs. 6 and 7a). Interactions extending over 6 or more rows apparently do not contribute significantly as the 6th, 7th and 8th coefficient are negligible both at low and high luminance.

3. Wide-Angle Interactions

The significance of wide-angle interactions can be examined in a more direct way by apparent-move-

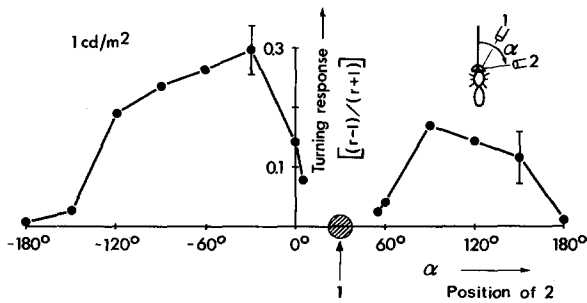


Fig. 8. Optomotor turning reactions induced by *straylight* (cf. text!). Each optic fibre (diameter 10 mm) subtends a visual angle of 15° in the equatorial plane of the fly's eye. The position of fibre 1 is fixed at 30° laterally (hatched disk) while the position of fibre 2 is varied (cf. inset). The intensity of the two circular spots is sinusoidally modulated at a frequency of 2 Hz. Phase shift 90° , 100% modulation, 1 cd/m^2 average luminance. A 100 W Xenon lamp with neutral density glass filters and a broad-band blue filter BG 23 is used as light source. Dark background. Responses (mean \pm S.E.M.) are obtained by a y-maze globe on 6 animals

ment experiments using two modulated light spots of variable angular separation.

At first sight the data in Fig. 8 seemed to dramatically contradict the above results (Fig. 7) as turning responses were measured at almost all values of the separation angle. However, when all receptors that were directly illuminated by one of the two light spots were occluded by black paint the responses were *not* abolished. Conversely, *zero* responses were obtained when two groups of receptors separated by more than 25° were stimulated by apparent movement using *optical imaging* of the light spots onto the retina. As this measure primarily reduces stray light, both control experiments indicate that *the responses of Fig. 8 are mediated by stray light* reaching zones of dark-adapted photoreceptors between those exposed to the two bright stimuli. All experiments with two discrete bright stimuli in front of a dark background were therefore carried out using optical imaging to eliminate the influence of stray light.

With this precaution the above experiment was repeated. Two narrow stripes were projected onto vertical rows of visual elements (Fig. 9). Positive responses are consistently measured for angular separations of less than 9° , in agreement with the previous conclusions (Figs. 6, 7). Beyond a separation of 10° , corresponding to 5 rows of visual elements, the reaction does not drop to zero but turns negative as has been observed previously on *Chlorophanus* (Hassenstein, 1958). Several properties of these negative responses have been determined to elucidate their possible origin and function. The negative responses are insensitive to the plane of polarization of the stimulus light and, near threshold intensity, they are optimally elicited at a contrast frequency of about 2 Hz similar to the positive responses (cf. Fig. 3) (Pick, unpublished results). In addition, the luminance threshold of the negative responses has been determined

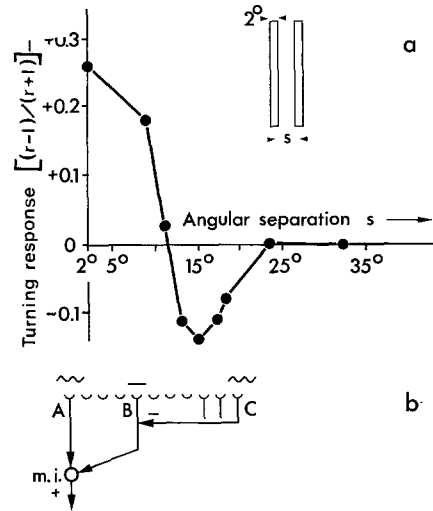


Fig. 9. **a** Turning responses of a single fly on the y-maze globe as a function of the angular separation s of two stripes which are each 2° wide and 40° high (stimulus 3). Modulation $\approx 100\%$, mean stimulus luminance $4 \cdot 10^{-3} \text{ cd/m}^2$. Dark background. In this eye region the angular separation $\Delta\varphi^*$ of neighbouring vertical rows of visual elements is 2° . **b** Schematic diagram to illustrate how the negative responses measured at $s > 12^\circ$ might be brought about in the case of a dark-adapted receptor at location B . Because of the inhibitory effect of receptor C on a unit at location B , the output of the movement-sensitive interaction (*m.i.*) is negative. If B receives modulated illumination (in the presence of gratings) or a sustained background light of 30% to 100% of the average brightness used to excite A and C , the effect of interaction AC is suppressed

(Fig. 10). In order to obtain more vigorous negative reactions the width of the two stripes has been increased to fill the entire field accessible through the microscope objective (diameter 40°) except for the dark bar which separates the two stripes (cf. inset Fig. 10). Comparison with Fig. 5 indicates a common luminance threshold for positive and negative responses (note that the stimulated field in the experiments of Fig. 5 was considerably larger). In view of the precaution taken by covering with black paint the ommatidia between those stimulated by the two stripes, this finding excludes that the negative responses might be caused by stray-light artefacts as were the responses of Fig. 8. The dependence of the negative responses in Fig. 10 on the width of the black bar between the two stripes may be readily explained when simple summation of the contributions from simultaneously stimulated "positive" and "negative" interactions is supposed. For example, with a 3.4° wide bar between the two stimulus components (and 3 rows of ommatidia covered – mind neural superposition) one may expect from the data of Fig. 9 positive contributions mainly from interactions between rows of visual elements 4° and 6° apart and negative contributions from rows 12° , 14° , 16° and 18° apart. These

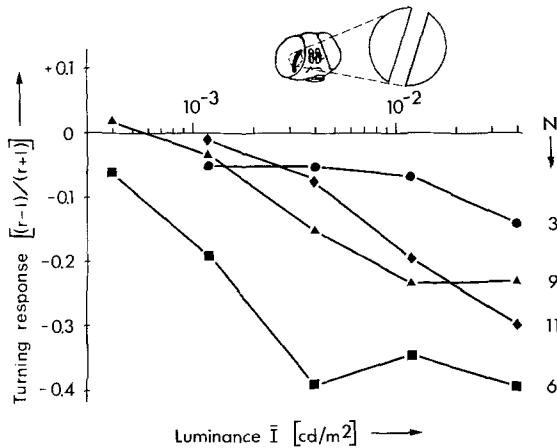


Fig. 10. Negative responses of a single fly on the y-maze globe to a wide-angle stimulus of apparent movement. Special care was taken to avoid stray-light effects by 1. stimulating through a microscope objective, 2. measuring near luminance threshold, 3. occluding a number (N) of vertical rows of ommatidia by black paint. The 40° aperture of the objective contains the two stimulus components which are separated by a dark bar of 3.4° , 8.0° , 13.5° , 17.5° width for $N=3, 6, 9, 11$, respectively. Stimulus frequency 2 Hz, modulation $\approx 100\%$

contributions result in a small negative response while with an 8° wide bar exclusively negative contributions sum to give a strong negative response. One final property of the negative responses has to be mentioned: They are abolished if the dark bar between the two flickering stripes is replaced by a stationary background light of 30 to 100% of the mean stimulus luminance. In the Discussion, these findings will be interpreted as an indirect manifestation of lateral inhibition.

Discussion

1. Temporal Adaptation

High grating speeds have been found to be ineffective movement stimuli at low luminance (Fig. 3). Luminance-dependent changes of the temporal modulation transfer have been established both for vertebrate and invertebrate photoreceptors: With increasing brightness, the high frequency crest becomes more pronounced and the low frequency tail is relatively attenuated. Estimates using the temporal modulation transfer of fly photoreceptors (Zettler, 1969) show that this change in receptor transfer may well account for the results presented in Fig. 3. Thus there is no need to assume any further neuronal mechanism of temporal adaptation.

2. The Spatial-Frequency Response $R(1/\lambda)$

The shape of the spatial-frequency response $R(1/\lambda)$ as measured in Figs. 6 and 7 is determined by three factors: (a) the spatial contrast transfer of the receptor system and mechanisms of luminance adaptation in the peripheral visual system, (b) the way in which movement is extracted from adjacent neuronal excitations, i.e., the intrinsic properties of the movement-specific interaction, and (c) the spatial connectivity pattern of the neural network underlying movement detection. In the following we consider how these three factors which are explicitly formulated in Eqs. (1) and (2) may be involved in the luminance-dependent modifications of the spatial-frequency function $R(1/\lambda)$.

(a) The light modulation in a receptor looking at a moving sine-wave grating depends on the spatial acceptance angle $\Delta\rho$ according to Eq. (2). Thus a luminance-dependent change in $\Delta\rho$ will necessarily alter the shape of the function $R(1/\lambda)$ (see below). Due to the parameter D , however, $R(1/\lambda)$ may change with luminance even if $\Delta\rho$ and the interaction coefficients $B_1, B_2 \dots$ are kept constant. At high luminance ($D \gg 1$) and high or moderate pattern contrast (e.g., $\Delta I/I \geq 40\%$) a twofold attenuation of the light modulation m_{rec} due to Eq. (2) will have very little effect on $R(1/\lambda)$ as the expression in square brackets of Eq. (1) is saturated (Fig. 2). When $D \ll 1$, on the other hand, $R(1/\lambda)$ will be attenuated approximately by a factor of 4 when m_{rec} is reduced to half. This example illustrates the necessity to determine the value of D prior to an analysis of $R(1/\lambda)$. From unpublished data on the contrast dependence of the optomotor response of *Musca* measured with stimulus set-up 2 we estimate that $D \approx 4$ and $D \approx 28$ at luminances of $\bar{I} = 3 \cdot 10^{-3} \text{ cd/m}^2$ and $\bar{I} = 10^2 \text{ cd/m}^2$, respectively. These values have been used in the calculation of the interaction coefficients (Fig. 7). The first five coefficients B_{1-5} are 0.151, 0.085, 0.033, 0.024, 0.016, and 0.064, 0.071, 0.068, 0.030, 0.034 [rev.r/rev.f] at high and low luminance, respectively. At low luminance, however, the value of D may vary from fly to fly by as much as a factor of 2 and since it was not possible in the present experiments to determine both D and $R(1/\lambda)$ for each individual fly, we have calculated the influence of such a variation on the interaction coefficients. The results show that the relative sizes of the first five coefficients B_{1-5} are essentially the same for $D=2$, $D=4$ and $D=8$.

Rigourously, Eq. (1) and its interpretation given here apply only when distortions of the hexagonal receptor array in the stimulated eye region are negligible and the stripes of the stimulus are aligned to the vertical rows of the array. These conditions can

be met satisfactorily only by stimulus set-up 2 (cf. methods). When nevertheless the data of Fig. 6 are analyzed according to Eq. (1) with $D \ll 1$ and $\Delta\rho = 2.4^\circ$ one obtains qualitatively similar interaction coefficients as in Fig. 7a. If on the other hand one tries to attribute the luminance dependent modification of $R(1/\lambda)$ solely to changes of the acceptance angle $\Delta\rho$, one has to postulate that $\Delta\rho$ increases with decreasing mean intensity by more than a factor of two which cannot be reconciled with any optical or electrophysiological data on the photoreceptors of *Musca*. Using the photopic interaction coefficients (inset Fig. 7b), $\Delta\rho \approx 6^\circ$ is the best value to transform the photopic shape of $R(1/\lambda)$ into the scotopic function, as indicated by the dashed curve in Fig. 6, whereas any figure of $\Delta\rho$ below 3.5° would be entirely inadequate. For the dark-adapted retinula cells R1-6 in the frontal eye of *Musca* a value of $\Delta\rho = 2.4^\circ$ has been previously measured by electrophysiological means (Scholes, 1969)².

(b) The intrinsic properties of the movement-specific interaction have been investigated for sinusoidal stimulation (Fig. 4). The sinusoidal shape of the response curve represents another experimental justification of (1) which derives the total response $R(1/\lambda)$ from a series of sine functions. Comparison of Fig. 4 with earlier data (Pick, 1974) indicates that, at least for sine-wave gratings which have been used throughout the present study, the characteristics of the movement-specific interaction itself remains unaffected by the average luminance and cannot serve to explain luminance-dependent modifications of $R(1/\lambda)$.

(c) It is therefore concluded that these modifications originate primarily from changes in the spatial interaction patterns. At different levels of luminance the various sampling bases are recruited with different weights as shown in Figs. 6 and 7a, b. The interaction coefficients have been calculated using a value of $\Delta\rho = 2.4^\circ$ (Scholes, 1969) but it should be mentioned that any value below 3° would not really alter the results. Activation of larger sampling bases obviously improves the detectability of coarse moving objects, while fine gratings in general become less detectable. In this sense, the data are interpreted as evidence for an adaptational mechanism which enhances sensitivity at the cost of spatial acuity.

Optomotor responses of flies as a function of the spatial wavelength λ of a periodic pattern have been obtained previously with flying animals (e.g., Götz 1964; Eckert, 1973). There is, however, one remark-

able difference to the present data. Yaw responses to square-wave gratings exhibit a "response plateau" which, in *Musca*, extends from $\lambda = 8^\circ$ to $\lambda = 360^\circ$ at high luminance and from $\lambda = 20^\circ$ to $\lambda = 360^\circ$ at very low luminance ($\bar{I} = 10^{-4}$ cd/m²) (Eckert, 1973). Walking responses to moving sine-wave gratings (Figs. 6 and 7) do not exhibit such a plateau. As the plateau is not found in flight experiments with sine-wave gratings (Pick, unpublished), it most likely is due to harmonics contained in the square-wave pattern. When a movement-detection system is well characterized by second-order nonlinearities, the contributions of the spatial Fourier components of the pattern to the response simply add. From Fig. 6 it is clear that the 3rd, 5th and 7th harmonics of a 360° square-wave pattern ($\lambda = 120^\circ$, 72° , and 51° , respectively) may appreciably contribute even if their amplitude is reduced to 1/3, 1/5 and 1/7 of the fundamental. At high luminance the plateau is probably extended to higher spatial frequencies due to saturation of the flight-motor system.

3. Neural Pooling or Movement-Specific Interactions

At this point we would like to add a note of caution on the interpretation of input-output experiments. By the formal analysis one may be tempted to identify each interaction coefficient in Figs. 6 and 7 with a proper movement detector in the nervous network. At low and high pattern luminance the various movement-specific signals could be weighted differently according to Figs. 6 and 7 prior to summation. Although this scheme is entirely feasible it is not the only possibility. Linear summation of input signals from neighbouring receptors *prior* to the (nonlinear) movement-specific interaction represents another plausible mechanism. It can account for the present data equally well when the summation extends over a receptive field of about 6° (cf. Fig. 6). A decision between the two alternatives or any combination thereof is theoretically not possible from the responses $R(1/\lambda)$ since the two interaction schemes lead to identical expressions in Eq. (1). It is mainly for this reason that we have not worked out a detailed two-dimensional map of spatial interactions which could be compared to earlier results on *Musca* (Kirschfeld, 1972; Kirschfeld and Lutz, 1974) and *Drosophila* (Buchner, 1976). It should be noted that, for the same argument, an analysis of the spike activity of a movement-sensitive interneuron cannot settle the question of whether the deterioration of spatial acuity at low luminance is a result of enhanced contributions from wide-angle movement detectors or of peripheral neural pooling (Dvorak and Snyder, 1978).

² We suppose that predominantly R1-6 mediate the low-luminance responses not only for reasons of the signal-to-noise ratio, but also because of the spectral sensitivity of the responses (Eckert, 1971) and their insensitivity to the plane of polarized light

4. On the Origin of the Negative Wide-Angle Responses

The results of the two-slits experiment (Fig. 9a) seem contradictory to the interpretation of $R(1/\lambda)$ (Fig. 7) in the sense that negative, wide-angle interactions appear under two-slit stimulation, but there is no indication of negative coefficients for the sampling bases $6\Delta\varphi^*$, $7\Delta\varphi^*$, $8\Delta\varphi^*$ derived from $R(1/\lambda)$. It was mentioned that the negative responses (Fig. 9a) are abolished when the ommatidia between those stimulated by the two slits receive a stationary background light. Thus the negative wide-angle interactions cannot be crucial for movement detection since they contribute to the response only under highly specific (and not very natural) stimulation of an otherwise dark-adapted retina. As shown in Fig. 9b, we suggest instead that such negative responses are brought about as an indirect by-product of lateral inhibition. $\Delta\varphi^*$, $2\Delta\varphi^*$, $3\Delta\varphi^*$, $4\Delta\varphi^*$ and $5\Delta\varphi^*$ are sampling bases (AB in Fig. 9b) available for movement-specific interactions (m.i.). The inhibition then (1) has to act on a dark-adapted unit at location B creating a 180° phase-shifted signal which interacts with the signal from A to give a negative response, (2) should extend – with decreasing strength – over at least 5 rows of ommatidia or 10° angular separation (cf. Fig. 10) and (3) should be essentially suppressed by a sustained light stimulus on photoreceptors at location B .

Monopolar cells in the lamina of *Calliphora* fulfill the first two properties (Zettler and Weiler, 1976; Mimura, 1976). It is unknown, however, whether the influence of the inhibitory surround of these cells flickered at 2 Hz, may be suppressed by a stationary centre stimulus of about equal average luminance. Even if the stationary excitation itself is not encoded in the monopolar cell *potential*, it could still cause the suppression by changing membrane *conductances*. At present it is not possible to relate the negative responses and their proposed interpretation by inhibition to the adaptational mechanisms discussed above. The suggestive possibility to identify neural pooling with reduced inhibition at low light levels must remain speculative as a quantitative comparison of behavioural responses under sinusoidal stimulation and electrophysiological responses to flash stimulation (Zettler and Weiler, 1976; Mimura, 1976) is not possible.

5. Scotopic Movement Detection

At low luminance the *absolute* sizes of the interaction coefficients strongly depend on the particular value of D used in the calculation (Eq. 1). For this reason the functional significance of the mechanism investigated here may be estimated only with help of an

additional assumption. We assume that the coefficient for nearest-neighbour interaction B_1 does not change with luminance. The data in Fig. 7 would support this assumption if $D=2$ was used instead of $D=4$ at low luminance. In terms of the proposed neuronal mechanisms this assumption means that increasing the weight of detectors with large sampling bases has no influence on the detectors with the smallest base or, alternatively, assuming that peripheral neural pooling is effected in such a way as not to increase the visual-field *overlap* of the two input elements to each movement detector. Using this assumption it may be calculated from Eq. (1) that the low-luminance responses to coarse gratings (e.g. $\lambda=45^\circ$) are enhanced by a factor of 2.2 due to the adaptational mechanism discussed here. With a criterion response of 50% “induced” and 50% random turns on the y-maze globe (0.5 on ordinate in Fig. 5), one may deduce from the threshold curves in Fig. 5 that the sensitivity of the actual system is improved by a luminance factor of about 2.5 compared to a non-adapting system. This gain factor should be compared to other sensitivity-improving mechanisms. The gain obtained by neural superposition for example is $\sqrt{6}$ (Kirschfeld, 1967; Smola, 1976). For the detection of narrow gratings on the other hand, the *non*-adapting system would be superior. Therefore the adaptational mechanism as described here is of particular advantage if the spatial frequency content of relevant visual objects is shifted to the low-frequency range which is equivalent to a shift of the visual “attention” from a distant to a closer-up surround. While visual cues from distant objects must be utilized for course control during flight, the reduced spatial resolution traded in for the gain in absolute light sensitivity may adapt the visual system to the spatial frequency range most relevant to an animal which has to grope its way at very low light levels.

We wish to thank H. Bülthoff, Drs. N. Franceschini, K.G. Götz, R. Hardie, K. Kirschfeld, T. Poggio, W. Reichardt and C. Wehrhahn for critically reading and discussing the manuscript. We are obliged to Miss C. Straub and M. Heusel for preparing the figures.

References

- Barlow, H.B.: Dark and light adaptation: psychophysics. In: Handbook of sensory physiology, Vol. VII/4. Visual psychophysics. Jameson, D., Hurvich, L.M. (eds.), pp. 1–28. Berlin, Heidelberg, New York: Springer 1972
- Buchner, E.: Elementary movement detectors in an insect visual system. *Biol. Cybernetics* **24**, 85–101 (1976)
- Buchner, E., Götz, K.G., Straub, C.: Elementary detectors for vertical movement in the visual system of *Drosophila*. *Biol. Cybernetics* **31**, 235–242 (1978)

- Collett, T.S., Land, M.F.: How hoverflies compute interception courses. *J. Comp. Physiol.* **125**, 191–204 (1978)
- Dvorak, D., Snyder, A.: The relationship between visual acuity and illumination in the fly, *Lucilia sericata*. *Z. Naturforsch.* **33c**, 139–143 (1978)
- Eckert, H.: Die spektrale Empfindlichkeit des Komplexauges von *Musca*. *Kybernetik* **9**, 145–156 (1971)
- Eckert, H.: Optomotorische Untersuchungen am visuellen System der Stubenfliege *Musca domestica* L. *Kybernetik* **14**, 1–23 (1973)
- Fermi, G., Reichardt, W.: Optomotorische Reaktionen der Fliege *Musca domestica*. *Kybernetik* **2**, 15–28 (1963)
- Götz, K.G.: Optomotorische Untersuchungen des visuellen Systems einiger Augenmutanten der Fruchtfliege *Drosophila*. *Kybernetik* **2**, 77–92 (1964)
- Hardie, R.C.: Electrophysiological analysis of fly retina. I: Comparative properties of R1–6 and R7 and 8. *J. Comp. Physiol.* **129**, 19–33 (1979)
- Hassenstein, B.: Ommatidienraster und afferente Bewegungsintegration. *Z. Vergl. Physiol.* **33**, 301–326 (1951)
- Hassenstein, B.: Über die Wahrnehmung der Bewegung von Figuren und unregelmäßigen Helligkeitsmustern. *Z. Vergl. Physiol.* **40**, 556–592 (1958)
- Heisenberg, M., Götz, K.G.: The use of mutations for the partial degradation of vision in *Drosophila melanogaster*. *J. Comp. Physiol.* **98**, 217–241 (1975)
- Heisenberg, M., Buchner, E.: The role of retinula cell types in visual behavior of *Drosophila melanogaster*. *J. Comp. Physiol.* **117**, 127–162 (1977)
- Kirschfeld, K.: Die Projektion der optischen Umwelt auf das Raster der Rhabdomere im Komplexauge von *Musca*. *Exp. Brain Res.* **3**, 248–270 (1967)
- Kirschfeld, K.: The visual system of *Musca*: Studies on optics, structure and function. In: Information processing in the visual system of arthropods. Wehner, R. (ed.), pp. 61–74, Berlin, Heidelberg, New York: Springer 1972
- Kirschfeld, K., Franceschini, N.: Optische Eigenschaften der Ommatidien im Komplexauge von *Musca*. *Kybernetik* **5**, 47–52 (1968)
- Kirschfeld, K., Lutz, B.: Lateral inhibition in the compound eye of the fly *Musca*. *Z. Naturforsch.* **29c**, 95–97 (1974)
- Land, M.F., Collett, T.S.: Chasing behaviour of houseflies (*Fannia canicularis*). *J. Comp. Physiol.* **89**, 331–357 (1974)
- Laughlin, S.B., Hardie, R.C.: Common strategies for light adaptation in the peripheral visual systems of fly and dragonfly. *J. Comp. Physiol.* **128**, 319–340 (1978)
- Mimura, K.: Some spatial properties in the first optic ganglion of the fly. *J. Comp. Physiol.* **105**, 65–82 (1976)
- Pick, B.: Visual flicker induces orientation behavior in the fly *Musca*. *Z. Naturforsch.* **29c**, 310–312 (1974)
- Pick, B.: Specific misalignments of rhabdomere visual axes in the neural superposition eye of dipteran flies. *Biol. Cybernetics* **26**, 215–224 (1977)
- Poggio, T., Reichardt, W.: Considerations on models of movement detection. *Kybernetik* **13**, 223–227 (1973)
- Reichardt, W., Poggio, T.: Visual control of orientation behaviour of the fly. *Q. Rev. Biophys.* **9**, (3), 311–438 (1976)
- Scholes, J.: The electrical responses of the retinal receptors and the lamina in the visual system of the fly *Musca*. *Kybernetik* **6**, 149–162 (1969)
- Smola, U.: Voltage noise in insect visual cells. In: Neural principles in vision. Zettler, F., Weiler, R. (eds.), pp. 194–213. Berlin, Heidelberg, New York: Springer 1976
- Snyder, A.W.: Acuity of compound eyes: physical limitations and design. *J. Comp. Physiol.* **116**, 161–182 (1977)
- Zettler, F.: Die Abhängigkeit des Übertragungsverhaltens von Frequenz und Adaptationszustand; gemessen am einzelnen Lichtrezeptor von *Calliphora erythrocephala*. *Z. Vergl. Physiol.* **64**, 432–499 (1969)
- Zettler, F., Weiler, R.: Neuronal processing in the first optic neuropile of the compound eye of the fly. In: Neural principles in vision. Zettler, F., Weiler, R. (eds.), pp. 227–237. Berlin, Heidelberg, New York: Springer 1976